Monte Carlo simulation study of the polymerization of polyurethane block copolymers: 3. Modelling of premature phase separation during reaction and differing reactivities of the chain extender and polyol using the simple sinking pool model

John A. Miller,* Thomas A. Speckhard,* James G. Homan and Stuart L. Cooper†

Department of Chemical Engineering, University of Wisconsin, Madison, Wisconsin 53706, USA

(Received 5 March 1986; revised 16 June 1986)

Because of the complexities involved in polyurethane reaction chemistry and the difficulties encountered in making experimental measurements, relatively little attention has been paid to determining the precise molecular weight, composition and hard-segment length distributions of polyurethane block copolymers. Yet, the available evidence suggests that variations in these distributions can markedly influence structure–property relationships in these materials. Therefore, computer models have been developed using Monte Carlo methods that allow for simulation of the polymerization process under various conditions and subsequent calculation of the various distributions. The model developed in this contribution is based on a sinking pool of monomers and is thus termed the simple sinking pool model. This model offers several advantages over previous models; in particular it can simulate effects due to differing reactivity of the chain extender and the polyol, and effects due to phase separation occurring at varying points in the reaction. The model and rationale behind the inclusion of the various parameters are described, and the effects of varying the model parameters on the simulated composition, molecular weight and hard-segment length distributions are determined and discussed.

(Keywords: Monte Carlo simulation; polyurethane; block copolymers; phase separation)

INTRODUCTION

Polyurethane block copolymers can be polymerized under a wide variety of conditions, leading to different molecular weight, hard-segment length and composition distributions[1–5]. The effects of changing these distributions on sample properties and morphology are not well understood because of the difficulties in obtaining accurate experimental characterization of the distributions[6–8] and because the complexity of the polyurethane reaction has hindered the development of a direct theoretical approach for calculating the various distributions under given polymerization conditions. Peebles[4,5] has shown that under certain ideal conditions the hard-segment length distribution should follow a most probable distribution. In the first contribution of this series[1], Peebles' ideal conditions and the assumption of a most probable distribution for the degree of polymerization in terms of hard and soft segments were used as the basis for a Monte Carlo model that calculated the corresponding composition and molecular weight distributions. In the second contribution of this series[2], the original model was modified to simulate premature phase separation during polymerization. Premature phase separation has been observed at the beginning of or at later points in bulk reactions by several investigators[9–14]. Depending on the particular system, the source of the phenomenon has been attributed to the incompatibility of the reactant monomers, incompatibility of the polymer and monomer, and crystallization of the polymer. In the modified model the reactants were partitioned into two phases at the start of the reaction and thus the model is best suited for the simulation of phase separation due to monomer incompatibility occurring immediately at the beginning of the reaction. The model showed how premature phase separation can lead to broader hard-segment length and molecular weight distributions and 'excess' compositional heterogeneity.

Both of the above models, the so-called single-phase and two-phase ideal reaction models, are termed ideal because they utilize the simplifying assumptions proposed by Peebles[4,5]. Several of the assumptions, in particular the equal reactivity of the chain extender and polyol hydroxyl groups and the equal reactivity of all isocyanate and hydroxyl groups regardless of the molecular weight of the growing chain, are likely to be poor approximations of actual behaviour under normal conditions especially in bulk polymerizations.

* Current address: 3M Research Center, St. Paul, MN 55144, USA.
† Author to whom correspondence should be addressed.

0032-3861/87/050758-10$03.00

Eisenbach[15] has recently shown that the distribution of products from the first step of a two-step bulk reaction does not follow the distribution predicted by Peebles. Therefore, the actual hard-segment length distribution will differ from that calculated using Peebles' approach. Although the hard-segment length, molecular weight and composition distributions calculated using the single-phase and two-phase ideal reaction models are useful for comparison purposes, it is clear that these models have several shortcomings for simulating the actual polymerization behaviour of polyurethane block copolymers. Therefore, in this contribution a different method, again based on a Monte Carlo simulation, is developed and described. This model, based on a sinking pool of monomers, is termed the simple sinking pool model and is described in the next section. The effects of varying the model parameters on the calculated hard-segment length, composition and molecular weight distributions are then described. The ability of all three models to simulate actual experimental data of MacKnight and coworkers on polybutadiene polyurethanes[9,10] will be evaluated and compared in the following contribution[16].

MODEL DESCRIPTION

The model described in this contribution, termed the simple sinking pool model, has three major improvements over the previous models. The first improvement is to allow for different effective reactivities for the chain extender and the polyol. The intrinsic rate constant[17] for each species reacting with an isocyanate group may be the same, but the effects of viscosity and diffusion may make the effective rate constants, especially in bulk reactions, different. The second advance allows for the simulation of phase separation occurring at various points and not just at the beginning of the reaction.

The third improvement over the previous models is in the use of a sinking pool of monomers for the Monte Carlo modelling. In the first two models, the chains were built up sequentially by whole segments from an infinite pool of segments. In this simulation the pool of monomers is finite; therefore, the simulation more accurately reflects the actual polymerization conditions. The probability of a given species being the next to react is not constant as in the first models, but depends on the number of that type of monomer remaining in the pool.

The various parameters used in the model, several of which are used to effect the improvements noted above, are described below:

Reaction stoichiometry. Molar ratios of diisocyanate/chain extender/polyol. The reaction need not be stoichiometric.

Types of monomers. A number of different typical reactants can be used.

Soft-segment molecular weight distribution. The polyol average molecular weight and distribution can be specified.

$\bar{D}_p$. The average degree of polymerization in terms of monomer units.

RCF. The reaction competitiveness factor, which is defined as the effective reactivity of the chain extender divided by the effective reactivity of the polyol. This quantity takes into account the differences in the intrinsic rate constants and the differences in the diffusivities of the chain extender and polyol.

SAF. The self-affinity factor, a parameter that is used to describe premature phase separation during the polymerization. Higher values of *SAF* correspond to greater incompatibility of the reactants and therefore a greater propensity for phase separation.

NSA. Degree of polymerization at which the effect of self-affinity begins. It has been noted by a number of workers[11-14] that phase separation often does not occur until a certain hard-segment length has been achieved. This parameter is used to describe this or similar situations.

Upper and lower D_p. Because of limitations on the computer, an upper limit for the degree of polymerization must be set. Practically this has liffle effect. The lower limit on the degree of polymerization can be used to model the effect of a precipitation step for a solution polymerization where the low molecular weight species are often lost.

Number of chains. The number of polymer chains to build up, typically 15 000.

Once the values for the above parameters are chosen, the model is then implemented in the following manner.

The first step is to set up three separate pools of monomers, one for each type, based on the stoichiometry, the average degree of polymerization and the total number of chains. A large array is then established where each row corresponds to one chain and each column to a monomer position. Within each row there will be a section of empty cells, a section of contiguous monomers that form the chain, then a final section of empty cells, so not all cells in the array will be filled with monomers at the end of the simulation process. The point within the row that the chain begins (the start of the polymerization process) is chosen at random so that the effect of depleting a monomer pool is not felt only by the chains with a large degree of polymerization. The degree of polymerization for each chain is also chosen at random such that the overall distribution of the degree of polymerization follows the most probable distribution and that the average value corresponds to that selected initially. The simulation proceeds in a stepwise parallel fashion, starting with the first column and continuing row by row. At the end of the column, the process continues on the subsequent column until the entire array has been operated on.

To visualize the simulation process, consider the cell in the array at (N,M), which corresponds to the Nth chain and the Mth position along the Nth row. We must first determine if the chain is growing at this point. If M is smaller than the point at which the chain begins or greater than the starting point plus the degree of polymerization of the Nth chain, nothing happens and we move on to the next cell. If not, the chain is growing and we must next determine what type of monomer is to be placed in this cell. If the previous cell $(N,M-1)$ contains a chain extender or a polyol, then this cell must receive a diisocyanate. If $(N,M-1)$ contains a diisocyanate, then a choice must be made between placing a chain extender in (N,M) or placing a polyol in (N,M). This choice is the key point in the simulation procedure.

The next step is to calculate the probability of adding a chain extender next (vs. polyol) based on several factors including the number of monomers of each type left in the pool (concentration), the reaction competitiveness factor

and self-affinity effects. Of these, the self-affinity effect requires the most calculation. If the current degree of polymerization of chain N is less than the value of the onset of self-affinity (*NSA*), we proceed directly to the calculation of the probability of reacting with a chain extender. Otherwise we look at the last five diol (chain extender (C) or polyol (P)) species that have been added to the chain. The most recent diol is assigned a value of 2.0, the second most recent 1.7, and the remainder 1.4, 1.2 and 1.0. These values are then summed for chain extender species and for polyols and 1.0 is added to each sum. These sums are then multiplied by the self-affinity factor (*SAF*). The basic concept behind this process is that a chain that has recently been adding primarily chain extenders is likely to be in a hard-segment-rich (chain-extender-rich) phase and is thus more likely to continue to add chain extenders. The reverse situation applies for chains that have recently been adding polyols. Thus if the last five diols in the chain are CCCCP and *SAF* is unity, the total self-affinity sum for the polyol would be 2.0, while for the chain extender it would be 7.3. These sums are then used in the calculation of the probability of reacting with a chain extender. (These sums are 1.0 when the chain D_p is less than *NSA*.) The probability of reacting with a chain extender is then given by:

$$P_C = \frac{N_C \times SA_C \times RCF}{N_C \times SA_C \times RCF + N_P \times SA_P}$$

where N_C and N_P are the number of chain extenders and polyols left in the pools, SA_C and SA_P are the sums for the self-affinity contributions and *RCF* is the reaction competitiveness factor. Based on this probability, either a polyol or a chain extender is placed in cell (N,M). The appropriate monomer pool is then depleted by one unit and this whole process is repeated for cell $(N+1,M)$.

After all of the cells in the array have been processed in the above fashion, the chain statistics are calculated. The polyol molecular weight is selected at random so that it conforms to the appropriate average and distribution. The hard-segment length, molecular weight and composition distributions are the main parameters that are tabulated during this step.

The second part of the modelling procedure for the simple sinking pool model involves a simulation of a solvent fractionation of a sample. Although, as noted in the first contribution of this series[1], the fractionation process probably depends on both the molecular weight and composition, in this step it is assumed that fractionation occurs only on the basis of composition. To simulate a fractionation where the soft-segment-rich fraction comprises 30% of the total weight of the polymer chains, the model starts with the chains with the lowest hard-segment content and sums their weight fraction until a value of 0.3 is reached. The average composition, $\bar{M}_n$ and $\bar{M}_w$ of this fraction are then calculated. Similar quantities are also calculated for the remaining hard-segment-rich fraction. The model can also calculate several fractionation points concurrently; these fractions are all calculated starting with the lowest hard-segment content species.

The simple sinking pool model is primarily intended for studying the premature phase separation phenomenon in a one-step bulk polymerization. However, the model can also be extended to other polymerization conditions. A one-step homogeneous solution polymerization can be modelled using the simple sinking pool model since it allows for differing rates of reaction of the polyol and the chain extender.

As currently implemented the model has several shortcomings. The model does not allow for unequal reactivity of the isocyanate groups on the diisocyanate, which will introduce some error in modelling a two-step reaction. The model assumes a most probable distribution (*MPD*) for the D_p distribution under conditions that should produce deviations from the *MPD*. It should be noted that there is presently no direct method for calculating what the D_p distribution should be under conditions where the reactivity of monomers varies throughout the reaction. It should be possible to calculate the D_p distribution under these conditions using an approach similar to Chaumont *et al.*[18] where the D_p of a chain is not predetermined and chains do not react only with monomers. Instead all species in the pool (i.e. dimers, trimers, etc.) can react with all other species. The model also ignores the effect of molecular weight on reactivity, and the modelling of phase separation by the self-affinity concept does not allow for different reaction rates in the two phases. Finally, the model allows for non-stoichiometric reaction conditions but does not include crosslinking effects. By combining and modifying the simple sinking pool method with some of the concepts and methods of the other approaches discussed previously[1,2,18] it is hoped that more realistic models can be developed. At this point the model is not intended to be an absolutely accurate description of polyurethane polymerizations but it can be utilized to achieve a qualitative understanding of the effects of various polymerization conditions on the resulting molecular weight, hard-segment length and composition distributions.

RESULTS AND DISCUSSION

For the purposes of comparison, a reference case is defined with the following characteristics and parameter values. The standard stoichiometry is defined as a 3/2/1 mole ratio of methylene bis(*p*-phenyl isocyanate) (MDI), butanediol (BD) and poly(tetramethylene oxide) (PTMO). The soft segment has a number average molecular weight of 1008 and a weight average molecular weight of 1450, with a molecular weight distribution described by the h.p.l.c. data reported by Miller *et al.*[19] The average degree of polymerization for the base case is 100, the *RCF* is 1 and no self-affinity is used. The lower bound for the degree of polymerization is 1 monomer unit and the upper bound is 1500. The number of chains used for the Monte Carlo simulation was fixed at 15 000.

The reference parameters (base case) for the sinking pool model produced the following molecular weight, hard-segment length and composition characteristics. The number average molecular weight was 31 850, the value of $\bar{M}_w/\bar{M}_n$ was 1.93, the hard-segment number average length (number of isocyanate units, $\bar{K}_n$) was 2.88 and the hard-segment K_w/K_n was 1.65 (K_w is weighted by the number of isocyanate units). The hard-segment fraction of the 10 wt% soft-segment-rich fraction was 0.372 and the 50 wt% soft-segment-rich fraction had a hard-segment fraction of 0.432. The total sample had a hard-segment weight fraction of 0.481. These values are

similar to the base case values for the single-phase ideal reaction model[1] ($\bar{M}_n = 28\,520$, $\bar{M}_w/\bar{M}_n = 1.96$, 0.369 and 0.430 hard-segment weight fractions for the 10 and 50 wt% soft-segment-rich fractions, and an overall hard-segment content of 48.1%). This agreement is not surprising since both cases have the same stoichiometry and soft-segment characteristics and do not include non-ideal effects. The differences between the models are due to the differences in the $\bar{D}_p$ values and how the degree of polymerization is defined as well as the use of a diisocyanate reactivity ratio (μ) of 3 in the calculation of the hard-segment distribution in the single-phase ideal reaction model. The net effect of these differences has been partially compensated for by choosing the base case $\bar{D}_p$ for the simple sinking pool model so that slightly higher molecular weight values, which lead to less compositional heterogeneity, are produced. The agreement between the two sets of base case values also indicates that the error involved in using a block degree of polymerization in the single-phase ideal reaction model instead of a D_p based on monomers does not significantly affect the composition and molecular weight distributions for the base value of the block degree of polymerization.

Varying the parameters common to both the single-phase ideal reaction model and the simple sinking pool model, such as the degree of polymerization, reaction stoichiometry, soft-segment molecular weight and molecular weight distribution and the limit of the lower degree of polymerization, leads to similar trends in the composition, hard-segment length and molecular weight distributions for the same reasons noted previously for the single-phase ideal reaction model[1]. Therefore, the discussion of results for these parameters will be limited to the effects of varying $\bar{D}_p$ and will include the effects on the hard-segment distribution which was fixed for a given stoichiometry and μ value in the single-phase reaction model.

Table 1 shows that increasing the value of D_p leads to an increase in the molecular weight and a decrease in the compositional heterogeneity, as expected. The compositional heterogeneity can be estimated using the fractional composition values for the 0.1 and 0.5 soft-segment-rich weight fractions. The more compositionally homogeneous the material, the closer the values for the hard-segment content of the soft-segment-rich fraction should approach the average hard-segment content of the sample. The effect of increasing $\bar{D}_p$ on the compositional heterogeneity can also be seen in *Figure 1*.

The abscissa in *Figure 1* is the cumulative weight fraction of chains in ascending order of hard-segment content. As the x value increases, the chains within an x interval possess a higher average hard-segment content than chains in previous x intervals. The ordinate is a measure of this change and is the fraction of hard-segment material in the chains within the specific x interval. This quantity is called the specific hard-segment weight fraction. Since a compositionally homogeneous sample would exhibit a horizontal line at the average composition value, these data clearly indicate the decrease in compositional heterogeneity with increasing $\bar{D}_p$. When comparing the data in the tables and figures it should be remembered that the fractional compositions in the tables are cumulative average values up to a certain cumulative weight fraction, whereas the figures are specific compositions at certain cumulative weight fraction intervals.

The effect of increasing $\bar{D}_p$ on the hard-segment distribution can be observed by examining the $\bar{K}_n$ and $\bar{K}_w/\bar{K}_n$ values in *Table 1* (number average and ratio of weight to number average hard-segment length in terms of isocyanate units) As $\bar{D}_p$ approaches ∞ (conversion goes to 100%) Peebles[4,5] showed that for a 3/2/1 stoichiometry under ideal conditions the values of $\bar{K}_n$ and $\bar{K}_w/\bar{K}_n$ should approach 3.0 and 1.66, respectively. The data in *Table 1* exhibit the expected behaviour but it is interesting to note that the large deviation at low $\bar{D}_p$ from the 100% conversion values, especially for $\bar{K}_n$.

The data in *Table* 1 also indicate that the $\bar{M}_w/\bar{M}_n$ values, which normally would be expected to increase with $\bar{D}_p$ actually decrease. The $\bar{N}_w/\bar{N}_n$ values, which are the ratio of the weight and number average degrees of polymerization, do increase and exhibit the values predicted by Flory[1,7]. This anomalous behaviour has been observed and explained previously[1] and is due to the

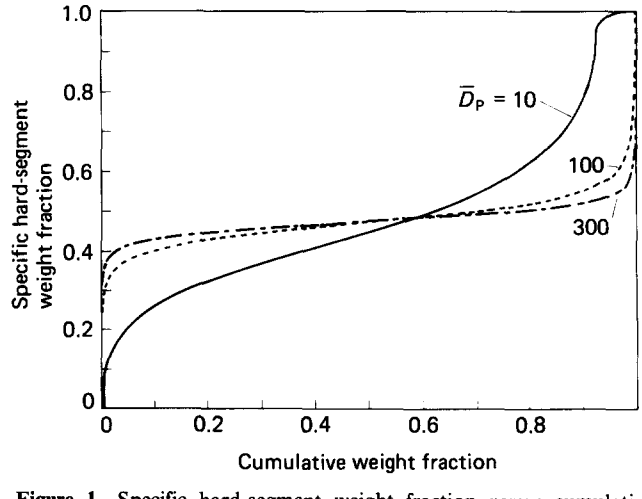

Figure 1 Specific hard-segment weight fraction *versus* cumulative weight fraction for the reference case with $\bar{D}_p = 10$, 100 and 300

Table 1 Effect of varying the degree of polymerization on the molecular weight, hard-segment length and composition distributions (3/2/1 MDI/BD/PTMO-1000(H), $RCF = 1.0$, no self-affinity)

$\bar{D}_p$	$\bar{M}_n$	$\bar{M}_w/\bar{M}_n$	$\bar{N}_w/\bar{N}_n$	Average composition	Fractional composition 0.1	Fractional composition 0.5	$\bar{K}_n$	$\bar{K}_w/\bar{K}_n$
5	1592	2.099	1.800	0.484	0.110	0.270	1.67	1.48
10	3224	2.038	1.900	0.483	0.197	0.333	2.14	1.57
50	15750	1.968	1.980	0.481	0.331	0.413	2.78	1.64
100	31850	1.934	1.990	0.481	0.372	0.433	2.88	1.65
300	91020	1.880	1.886	0.481	0.414	0.452	2.96	1.66

fact that the monomers do not all have the same molecular weight and the fact that a finite array is used to represent the D_p distribution.

Table 2 shows the effect of having a non-stoichiometric reaction (which was not allowed in the previous models) on the various distributions. Part (a) of the table uses a degree of polymerization that is the maximum for a given stoichiometry while part (b) of the table holds the degree of polymerization constant as the stoichiometry is changed. The effect of changing the stoichiometry is very small, except in cases (part (a)) where the stoichiometry will limit the average degree of polymerization significantly, in which case the influence of changes in $\bar{D}_p$ will dictate the behaviour of the molecular weight and distribution and the compositional heterogeneity. For typical bulk polymerization processes, where only a few per cent excess diisocyanate is used, the influence of the non-stoichiometric conditions will be minimal. The above discussion, of course, neglects any effect due to crosslinking, which is likely to occur in systems with excess diisocyanate.

To this point only reaction conditions which affect the natural heterogeneity of a system have been discussed. The first factor that leads to excess compositional heterogeneity is the unequal effective reactivities of the polyol and the chain extender. *Table 3* shows the effect of changing the *RCF* for the 3/2/1 MDI/BD/PTMO system. The number average molecular weight of the polymer is unaffected by *RCF*, as expected. However, as the *RCF* deviates from a value of 1, the breadth of the molecular weight distribution as measured by $\bar{M}_w/\bar{M}_n$ increases substantially. The effect on $\bar{M}_w/\bar{M}_n$ is greater for variations in *RCF* than for any of the factors that only affect the natural compositional heterogeneity. A similar situation exists for the hard-segment length distribution. The average length ($\bar{K}_n$) does not change appreciably with changes in the reaction competitiveness factor, but as the *RCF* deviates from 1, the value of $\bar{K}_w/\bar{K}_n$ increases. For the compositional heterogeneity, again the same situation exists in that as the *RCF* deviates from unity, the difference between the average and fractional composition increases. The increase in compositional heterogeneity can be seen in *Figures 2a* to *2c*, which show three-dimensional histograms of composition and molecular weight on the x-axis and y-axis while the z-axis represents the relative number of chains with compositions and molecular weight values corresponding to that section of the grid. As the *RCF* increases from 0.1 to 1.0, the molecular weight–composition data shift towards a more homogeneous system. As the *RCF* increases further, the system becomes more heterogeneous.

The effect of varying *RCF* on the composition distribution can also be seen in *Figure 3*. For $RCF = 1$ the composition curve exhibits a shape typical of an ideal system with some natural heterogeneity[1]. When $RCF = 0.1$ the system becomes much more heterogeneous and the composition curve is no longer symmetric, indicating the presence of non-ideal effects. In particular, there is a large fraction of material that is almost pure hard segment. This is because when $RCF = 0.1$, most of the polyol reacts early in the reaction, depleting the pool of polyol, and thus chains reacting towards the end of the polymerization are almost entirely isocyanate and chain extender. The opposite situation occurs when $RCF = 10.0$, but since there is always some isocyanate in a chain (unless $D_p = 1$) there is little pure soft-segment material. Note, however, that the average hard-segment content of the most soft-segment-rich material does decrease. Finally, it is obvious that the fractional

Table 2 Effect of having non-stoichiometric reaction conditions on the molecular weight, hard-segment length and composition distributions (*A*/2/1 MDI/BD/PTMO-1000(H), $RCF = 1.0$, no self-affinity)

	Moles of MDI (*A*)	$\bar{D}_p$	$\bar{M}_n$	$\bar{M}_w/\bar{M}_n$	Average composition	Fractional composition 0.1	Fractional composition 0.5	$\bar{K}_n$	$\bar{K}_w/\bar{K}_n$
(a) Degree of polymerization is maximum for stoichiometry	3.05	120	37640	1.930	0.483	0.385	0.439	2.90	1.65
	3.10	60	18930	1.964	0.487	0.352	0.425	2.81	1.64
	3.20	30	9512	1.999	0.494	0.316	0.406	2.66	1.61
	3.30	20	6306	2.003	0.499	0.287	0.390	2.52	1.59
	3.50	12	3778	2.038	0.513	0.255	0.372	2.30	1.55
(b) $\bar{D}_p$ fixed at 30	3.00	30	9570	1.963	0.481	0.292	0.394	2.64	1.62
	3.05	30	9518	1.983	0.484	0.302	0.398	2.65	1.63
	3.10	30	9557	1.979	0.488	0.306	0.401	2.65	1.62
	3.20	30	9512	1.999	0.494	0.316	0.406	2.66	1.61

Table 3 Effect of varying the reaction competitiveness factor (*RCF*) on the molecular weight, hard-segment length and composition distributions (3/2/1 MDI/BD/PTMO-1000(H), $\bar{D}_p = 100$, no self-affinity)

RCF	$\bar{M}_n$	$\bar{M}_w/\bar{M}_n$	Average composition	Fractional composition 0.1	Fractional composition 0.5	$\bar{K}_n$	$\bar{K}_w/\bar{K}_n$
0.1	31730	2.309	0.481	0.223	0.266	2.86	11.6
0.2	31730	2.189	0.481	0.257	0.308	2.87	6.86
0.5	31730	2.034	0.481	0.326	0.385	2.87	2.28
1.0	31850	1.934	0.481	0.372	0.433	2.88	1.65
2.0	31380	1.946	0.481	0.259	0.379	2.90	1.91
5.0	31650	2.134	0.481	0.192	0.282	2.91	2.96
10.0	31650	2.281	0.481	0.185	0.237	2.91	4.43

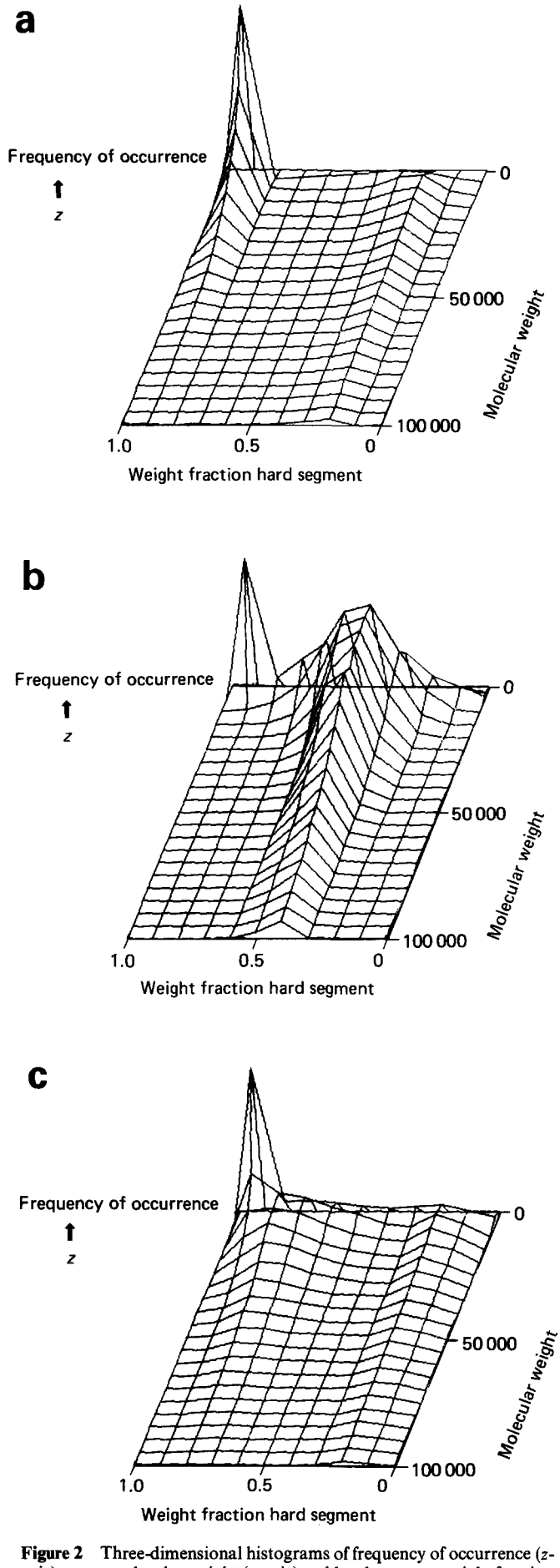

Figure 2 Three-dimensional histograms of frequency of occurrence (z-axis) *versus* molecular weight (y-axis) and hard-segment weight fraction (x-axis) for the reference case with $RCF = 0.1$ (a), $RCF = 1$ (b) and $RCF = 10$ (c)

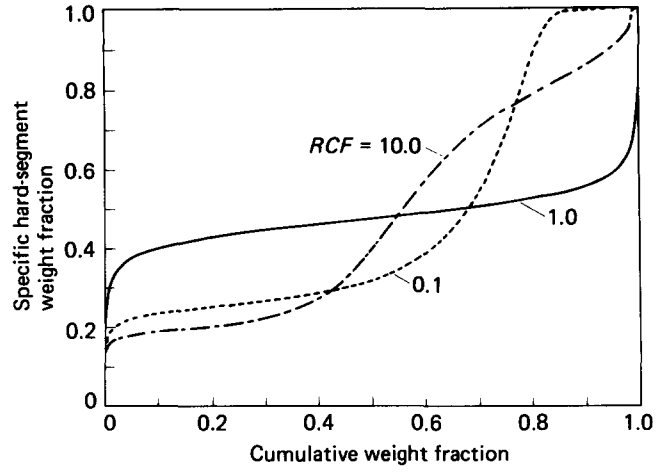

Figure 3 Specific hard-segment weight fraction *versus* cumulative weight fraction for the reference case with $RCF = 0.1$, 1 and 10

composition data presented in *Table 3* do not necessarily indicate which sample is more compositionally heterogeneous when non-ideal effects are being considered because the composition curves are no longer symmetric. For example, the data in *Table 3* would indicate that an RCF of 10 leads to greater compositional heterogeneity than an RCF of 0.1, but, as noted previously[2], this is because these data are sensitive to the fraction of material that is very rich in soft segments, corresponding to the left-hand portion of *Figure 3*.

The effect of RCF on the hard-segment length distribution can be seen in *Figures 4a* to *4c*. A histogram of weight fraction (number fraction weighted by the length of the hard segment) *versus* length of the hard segment (number of diisocyanate units) is shown in *Figure 4a* for an $RCF = 1.0$, which results in a most probable distribution (MPD) as indicated by Peebles[4,5]. (There is a slight deviation from an MPD because the conversion is not 100%.) *Figures 4b* and *4c* show the distribution for values of $RCF = 0.1$ and 10, respectively. In both cases there are more longer and more shorter hard segments than is the case for the MPD. Comparing the data in *Figures 4b* and *4c* indicates that fewer single unit hard segments are produced when $RCF = 0.1$ than when $RCF = 10$. When $RCF = 10$ the chain extender pool becomes depleted during the reaction and thus the remaining hard segments must be one diisocyanate unit long. When $RCF = 0.1$ it is favourable to form hard segments that are only one unit long early in the reaction, but there is always a finite chance of forming longer hard segments. Thus, fewer one-unit-long hard segments but more two-units-long hard segments are formed when $RCF = 0.1$ as compared with $RCF = 10$. The situation is reversed for long hard segments. Although the data shown in *Figures 4b* and *4c* do not extend out to high enough hard-segment lengths for the effect to be observed, the case with $RCF = 0.1$ actually has more very long hard segments than the case with $RCF = 10$ (weight fractions are less than 0.0003 for hard-segment lengths greater than 66 when $RCF = 10.0$ but not until hard-segment lengths are greater than 148 for $RCF = 0.1$). The large effect on $\bar{K}_w$ due to very long hard segments is reflected in the larger $\bar{K}_w/\bar{K}_n$ values for $RCF = 0.1$ compared with $RCF = 10.0$ in *Table 3*.

The other factor that can cause excess compositional heterogeneity is the self-affinity factor (SAF) which is used

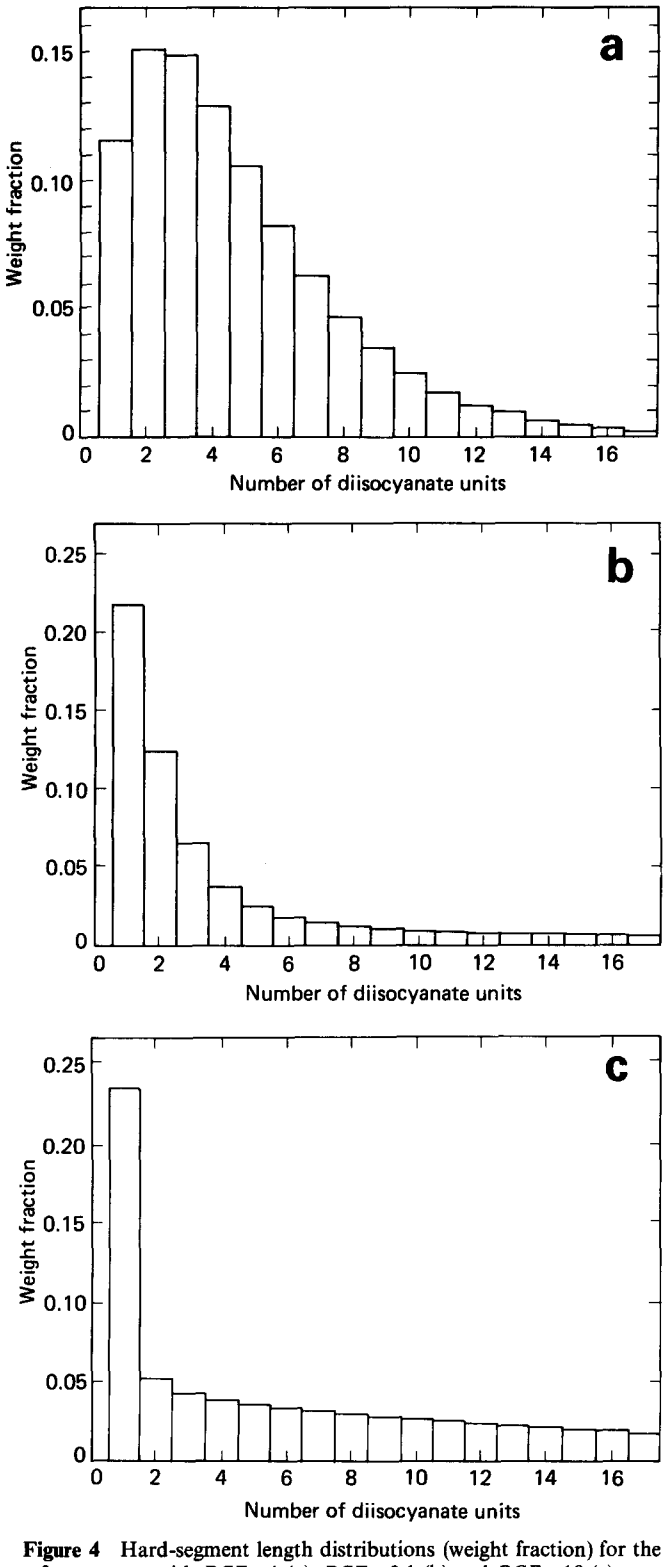

Figure 4 Hard-segment length distributions (weight fraction) for the reference case with $RCF = 1$ (a), $RCF = 0.1$ (b) and $RCF = 10$ (c)

to model phase separation. *Table 4a* shows the effect of changing the self-affinity factor on the molecular weight and distribution, the hard-segment molecular weight distribution and the compositional heterogeneity. The stoichiometry for these simulations was 3/2/1, the degree of polymerization was 100 and the *RCF* was unity. Additionally, the D_p value for a given chain at which self-affinity effects begin (*NSA*) was fixed at 10. $\bar{M}_n$ and $\bar{K}_n$ are unaffected by the changes in the *SAF*, as expected. As the *SAF* increases, the molecular weight distribution of the whole polymer becomes broader as does the hard-segment length distribution. The data in *Table 4a* and in *Figure 5* show that the compositional heterogeneity also increases significantly as the *SAF* is increased. *Figures 6a* and *6b* show three-dimensional histograms for the cases where the self-affinity factor is 1 and 10 respectively. The three-dimensional histogram for the case where the *SAF* is zero was shown in *Figure 2b*. The central ridge in *Figure 2b* spreads out in *Figure 6a* and spreads even further in *Figure 6b*, indicative of a broadening of the distribution of compositions at all molecular weights as the *SAF* is increased. These effects are expected since, as the *SAF* rises, the tendency for chains to propagate with the same type of segment increases, leading to broader hard-segment length, composition and molecular weight distributions.

Part (b) of *Table 4* shows the effect of varying the D_p value at which self-affinity effects begin (*NSA*) in an individual chain at a constant *SAF* value. Varying the *NSA* value can be done effectively to simulate phase separation occurring at different points in a reaction. As *NSA* increases, phase separation would effectively occur later and its influence on molecular characteristics would be diminished. Thus, as *NSA* increases, effects due to self-affinity decrease, as evidenced by the data in *Table 4b*. Note in particular the large decrease in $\bar{K}_w/\bar{K}_n$ values as *NSA* increases.

The results from *Tables 3* and *4* indicate that the effects on the various distributions of the *RCF* and *SAF* are quite similar. This is not surprising since each factor effectively functions by depleting one of the monomer pools. Thus, if one were to evaluate actual experimental data it would be practically impossible without additional information (e.g. phase separation did not occur) to distinguish between effects due to unequal reactivity or phase separation. However, the physical bases for these effects are independent and with a different type of model, for example where phase separation is modelled by partitioning, it should be possible to separate the effects.

Table 5 shows the behaviour of systems where both the self-affinity factor (*SAF*) and the reaction competitive ness factor (*RCF*) are varied. As expected, these two effects can influence each other markedly since each mechanism attempts to deplete one of the monomer pools and thus competes for effect. At larger *SAF* values,

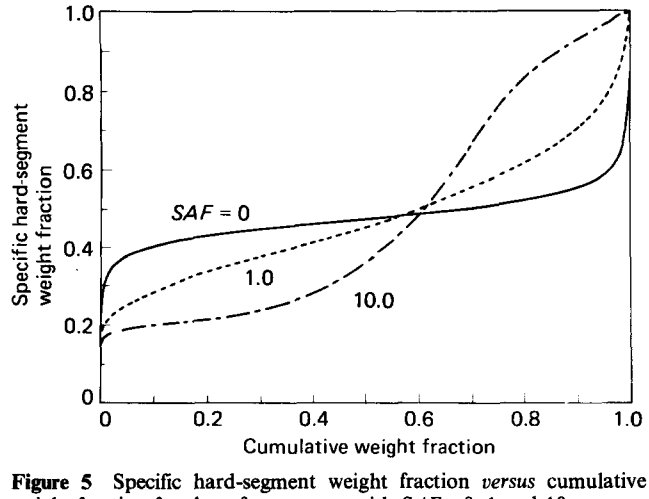

Figure 5 Specific hard-segment weight fraction *versus* cumulative weight fraction for the reference case with $SAF = 0$, 1 and 10

Table 4 Effect of varying the self-affinity factor (*SAF*) and the D_p at which self-affinity effects begin (*NSA*) on the molecular weight, hard-segment length and composition distributions (3/2/1 MDI/BD/PTMO-1000(H), $\bar{D}_p = 100$, $RCF = 1.0$)

	SAF	*NSA*	$\bar{M}_n$	$\bar{M}_w/\bar{M}_n$	Average composition	Fractional composition 0.1	Fractional composition 0.5	$\bar{K}_n$	$\bar{K}_w/\bar{K}_n$
(a)	0	–	31850	1.934	0.481	0.372	0.433	2.88	1.65
Constant	0.1	10	31240	1.903	0.480	0.347	0.421	2.88	1.89
NSA	0.5	10	31640	1.946	0.480	0.289	0.382	2.89	2.90
	1.0	10	31380	1.992	0.480	0.252	0.353	2.89	4.06
	2.0	10	31430	2.023	0.481	0.224	0.322	2.89	5.97
	5.0	10	31720	2.124	0.481	0.201	0.276	2.89	10.1
	10	10	31710	2.211	0.481	0.195	0.244	2.89	13.4
	100	10	31630	2.477	0.481	0.188	0.207	2.89	19.8
(b)	10	1	31810	2.020	0.480	0.183	0.237	2.89	15.2
Constant	10	3	31920	2.162	0.480	0.185	0.236	2.89	14.5
SAF	10	5	31240	2.208	0.480	0.187	0.236	2.89	13.6
	10	10	31710	2.211	0.481	0.195	0.244	2.89	13.4
	10	50	31730	2.015	0.480	0.226	0.306	2.89	10.0
	10	100	31000	1.868	0.480	0.265	0.360	2.89	6.84

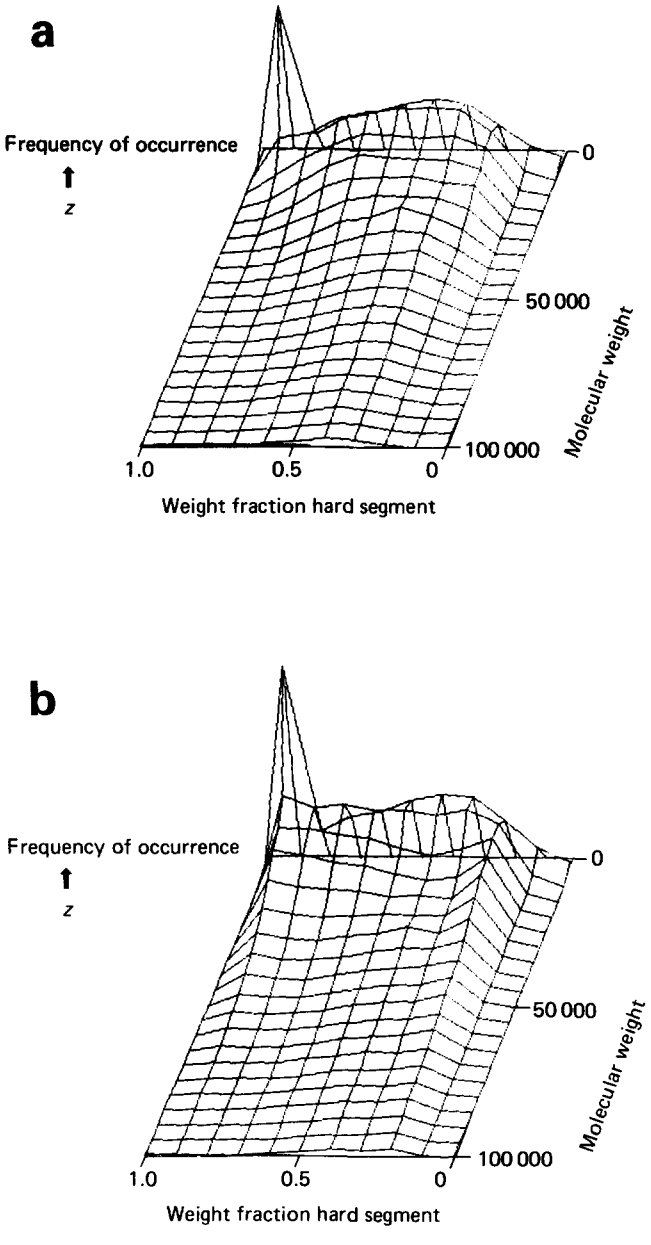

Figure 6 Three-dimensional histograms of the molecular weight, the weight fraction of hard segment and the relative frequency of occurrence for the reference case with $SAF = 1$ (a) and $SAF = 10$ (b)

changes in *RCF* produce smaller changes in the whole chain and hard-segment molecular weight distributions and the compositional heterogeneity. Similarly, as the *RCF* deviates from unity, the effect of changes in the *SAF* on the various distributions is diminished. Nevertheless, when *RCF* deviates from 1 and *SAF* is greater than zero, very broad hard-segment length and composition distributions can be obtained as indicated by the data in *Table 5* and *Figure 7*. Note that the composition distribution in *Figure 7* is what one would expect from a blend of two materials with a large difference in hard-segment contents and is similar to those obtained using the two-phase ideal reaction model[2].

Table 6 shows the effect of varying the degree of polymerization under various non-ideal conditions (the effects of varying $\bar{D}_p$ under ideal conditions ($RCF = 1$, $SAF = 0$) were shown in *Table 1* and *Figure 1*). The same trends noted in *Table 1* are observed; as $\bar{D}_p$ increases, $\bar{M}_w/\bar{M}_n$ and the compositional heterogeneity decrease, while $\bar{K}_w/\bar{K}_n$ increases. What is somewhat surprising are the large changes in $\bar{K}_w/\bar{K}_n$ as $\bar{D}_p$ is varied. The large variability in $\bar{K}_w/\bar{K}_n$ is due to the fact that at higher $\bar{D}_p$ values there are more monomers in the pool thereby allowing for greater depletion effects, and because the effect of limited chain length restricting hard-segment lengths is reduced. Thus, increasing $\bar{D}_p$ tends to accentuate the effects of varying *SAF* and *RCF* on the hard-segment length distribution but reduces the effect on the composition and molecular weight distributions.

Finally, it should be noted that while the effects of varying *SAF* and *NSA* (and also *RCF*) can produce results for the various distributions similar to those obtained using the two-phase ideal reaction model[2], there are distinct differences between the models particularly in obtainable molecular weight distributions. These differences become apparent when the various models are used to simulate experimental data and will be discussed in the following contribution[16].

SUMMARY

An alternative Monte Carlo method has been developed and described that involves the use of a sinking pool of monomers and allows for calculation of the molecular weight, hard-segment length and composition distri-

Table 5 Effect of varying the reaction competitiveness factor (*RCF*) and the influence of the self-affinity factor (*SAF*) on the molecular weight, hard-segment length and composition distributions (3/2/1 MDI/BD/PTMO-1000(H), $\bar{D}_p = 100$)

RCF	*SAF*	$\bar{M}_n$	$\bar{M}_w/\bar{M}_n$	Average composition	Fractional composition		$\bar{K}_n$	$\bar{K}_w/\bar{K}_n$
					0.1	0.5		
0.1	0.1	31730	2.330	0.481	0.214	0.255	2.86	11.1
0.1	1.0	31730	2.390	0.481	0.195	0.229	2.86	10.1
0.1	10.0	31640	2.529	0.481	0.186	0.208	2.86	17.0
1.0	0.1	31240	1.903	0.480	0.347	0.421	2.88	1.89
1.0	1.0	31380	1.992	0.480	0.252	0.353	2.89	4.06
1.0	10.0	31710	2.211	0.481	0.195	0.244	2.89	13.4
10.0	0.1	31650	2.332	0.481	0.184	0.225	2.91	5.87
10.0	1.0	31650	2.440	0.481	0.184	0.211	2.92	12.0
10.0	10.0	31440	2.438	0.481	0.180	0.201	2.92	18.9

Table 6 Effect of varying degree of polymerization (D_p) on the influence of the reaction competitiveness factor (*RCF*) and the self-affinity factor (*SAF*) on the molecular weight, hard-segment length and composition distributions (3/2/1 MDI/BD/PTMO-1000(H), $NSA = 10$)

$\bar{D}_p$	*RCF*	*SAF*	$\bar{M}_n$	$\bar{M}_w/\bar{M}_n$	Fractional composition		$\bar{K}_n$	$\bar{K}_w/\bar{K}_n$
					0.1	0.5		
10	0.1	0	3190	2.408	0.167	0.245	2.04	2.40
100	0.1	0	31730	2.309	0.223	0.266	2.86	11.6
300	0.1	0	92210	2.044	0.238	0.297	2.95	21.95
10	10	0	3173	2.362	0.126	0.223	2.29	2.22
100	10	0	31650	2.281	0.192	0.282	2.91	2.96
300	10	0	90990	2.046	0.194	0.286	2.97	5.01
10	1	1	3201	2.043	0.169	0.296	2.16	2.04
100	1	1	31380	1.992	0.252	0.353	2.89	4.06
300	1	1	90910	1.902	0.297	0.386	2.96	4.55

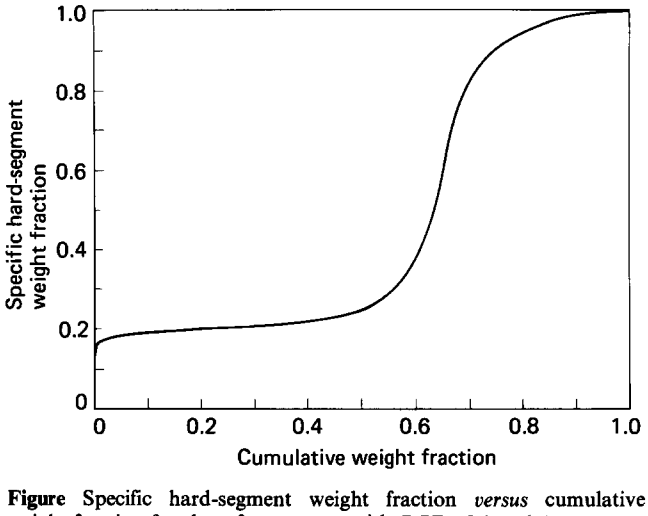

Figure Specific hard-segment weight fraction *versus* cumulative weight fraction for the reference case with $RCF = 0.1$ and $SAF = 10$

butions of polyurethane block copolymers under various polymerization conditions. This model offers several advantages over previous approaches, including the ability to model different reactivities of the chain extender and polyol and phase separation at various points in the reaction. Varying parameters, such as the degree of polymerization, soft-segment molecular weight distribution and hard-segment content, that only affect the natural heterogeneity produced effects on the molecular weight and composition distributions similar to those described previously[1]. The effects of varying the reaction competitiveness factor (*RCF*), which was used to simulate differing reactivities of chain extender and polyol, and the self-affinity factor (*SAF*), which was used to model phase separation, were similar. Increasing *SAF* values or increasing the deviation of *RCF* from 1 led to a much broader hard-segment length distribution, increased compositional heterogeneity and a broader molecular weight distribution. The effects of varying *SAF* were also influenced by the choice of the degree of polymerization at which self-affinity effects begin (*NSA*). Higher *NSA* values correspond to phase separation occurring later in the reaction and resulted in a reduced influence of self-affinity on the various distributions. When both *SAF* and *RCF* deviate from ideal conditions the total effect will be less than the sum of the two individual effects since each mechanism can serve to deplete one of the monomer pools, and thus the two effects are competitive.

ACKNOWLEDGEMENTS

The authors would like to acknowledge partial support of this research by the National Science Foundation, Division of Materials Science, Polymer Section, Grant No. DMR 86-03839 and through a grant from the Office of Naval Research.

REFERENCES

1 Speckhard, T. A., Miller, K. A. and Cooper, S. L. *Macromolecules* 1986, **19**, 1558
2 Miller, J. A., Speckhard, T. A. and Cooper, S. L. *Macromolecules* 1986, **19**, 1568
3 Saunders, J. H. and Frisch, K. C. 'Polyurethane Chemistry and Technology: Part I, Chemistry', Interscience, New York,, 1962

4 Peebles, L. H. *Macromolecules* 1974, **7**, 872
5 Peebles, L. H. *Macromolecules* 1976, **9**, 58
6 Lee, D. C., Speckhard, T. A., Sorenson, A. D. and Cooper, S. L. *Macromolecules* 1986, **19**, 2383
7 Speckhard, T. A. and Cooper, S. L. *Rubber Chem. Technol.* 1986, **59**, 405
8 Speckhard, T. A. Ph.D. Thesis, University of Wisconsin–Madison, 1985
9 Xu, M., MacKnight, W. J., Chen, C. H. Y. and Thomas, E. L. *Polymer* 1983, **24**, 1327
10 Chen, C. H. Y., Briber, R. M., Thomas, E. L., Xu, M. and MacKnight, W. J. *Polymer* 1983, **24**, 1333
11 Castro, J. M., Lopez-Serrano, F., Camargo, R. E., Macosko, C. W. and Tirrell, M. *J. Appl. Polym. Sci.* 1981, **26**, 2067
12 Castro, J. M., Macosko, C. W. and Perry, S. J. *Polymer* 1984, **25** (*Commun.*), 83
13 Hagar, S. L., MacKury, T. B., Gerkin, R. M. and Critchfield, R. F. *ACS Adv. Chem. Ser.* 1981, **172**
14 Camargo, R. E. Ph.D. Thesis, University of Minnesota, 1983
15 Eisenbach, C. D. *ACS Polym. Prepr.* 1985, **26**(2), 7
16 Speckhard, T. A., Homan, J. G., Miller, J. A. and Cooper, S. L. *Polymer* 1987, **28**, 768
17 Flory, P. J. 'Principles of Polymer Chemistry', Cornell University Press, Ithaca, NY, 1953
18 Chaumont, P., Gnanou, Y., Hild, G. and Rempp, P. *Makromol. Chem.* 1985, **186**, 2321
19 Miller, J. A. and Cooper, S. L. *Makromol. Chem.* 1984, **185**, 2429